UDC 532.542
DOI: 10.18372/2310-5461.34.11615

A. O. Borysyuk,
Ya. A. Borysyuk
Institute of Hydromechanics of the National Academy of Sciences of Ukraine
aobor@ukr.net
0000-0002-3878-3915

WALL PRESSURE FLUCTUATIONS BEHIND A PIPE NARROWING OF VARIOUS SHAPES

Introduction

Local stenotic narrowings of blood vessels are often the reason for serious circulatory disorders. They can result in ischemia of body organs and tissues, high blood pressure, production of blood clots, etc. [1, p. 347; 2, p. 475; 3, p. 658]. As the clinical studies show, the stronger the stenosis the more severe is the disease caused by it. Therefore, the detection of a stenosis at an early stage in its development is an important practical problem.

The most popular method for obtaining information about a stenosis is arteriography. It is based on the injection of a roentgen-contrast fluid into the artery via a catheter, the formation of an X-ray-image of the region of interest, and subsequent study of that image in order to determine the degree of vessel obstruction. However, this technique is invasive, uncomfortable for the patient, involves a risk of infection, bleeding and arrhythmia, etc. and is usually only used when a stenosis results in serious clinical symptoms [3, p. 659].

In such a situation, developing *non-invasive* diagnostic methods for finding a stenosis from an analysis of changes in the dynamic and/or acoustic characteristics of the associated blood flow is of great concern to the medical clinician. The method of phonoangiography occupies a special place among such techniques [3, p. 659]. It requires the availability of appropriate information about the mechanisms of vascular sound generation and transmission to the body surface, as well as the various factors which affect them.

With these known, a model of the appropriate vascular district can be developed and used to predict the relationships between the characteristics of the acoustic field heard at the body surface and the parameters of the vessel and the flow. These relationships can then be applied to find a stenosis from the corresponding changes in the acoustic field structure.

An adequate description of the flow and the noise sources (i.e., the wall pressure fluctuations, p_t) behind a stenosis is one of the key factors in the method of phonoangiography. As analysis of the literature shows, the spatial structure of both the flow and the pressure p_t behind a narrowing of the simplest shapes has been investigated rather well. In particular, the disturbed flow region behind a narrowing has been found. It has been characterised as follows. First, a separation region (with recirculating flow between the jet and the vessel wall) is usually observed. It is followed by a reattachment region, and finally by flow stabilization and recovery to the state upstream of the narrowing [3, p. 659]. The flow centerline velocity in the flow separation and flow reattachment domains remains almost unchanged from its value in the narrowing throat [3, p. 659]. The *rms* (i.e., root-mean-square) wall pressure is characterised by a sharp increase in these domains, and reaches a maximum before the flow reattachment point [3, p. 659]. There are also approximate estimates for the upper limits of the lengths of the flow regions identified above, as well as quantitative relationships relating both the distance from a narrowing to the point of maximum *rms* pressure and the *rms* magnitude at this point to the parameters of the flow, vessel and narrowing [3, p. 660]. However, the appropriate estimates and relationships of different authors differ from each other, even for identical narrowing geometries.

Unlike the spatial characteristics of the pressure p_t behind a narrowing, its spectral characteristics have been investigated rather little. A few works can be found, in which only the general shape of its power spectrum has been obtained, and the qualitative dependence of the spectrum level on the flow Reynolds number and the narrowing severity has been analysed. More specific features of the spectrum (such as local maxima, slope of the

spectral curve, etc.) and their relation to the vortices behind a narrowing, as well as variation of the spectrum with axial distance from the narrowing were either not found or given insufficient attention by investigators. However, these details are important for analysis of the corresponding acoustic field [2, p. 476; 3, p. 660]. Furthermore, no studies of the effects of narrowing shape parameters on the wall pressure characteristics are available. The lack of information about the spectral structure of the pressure p_t, the effects of the narrowing shape parameters, as well as the absence of universal estimates and relationships for the spatial characteristics of p_t, stimulated this investigation.

Experiment

To make the investigation, a suitable experimental system has been developed. A detailed description of the system is given in [3, pp. 660. 661], and we restrict ourselves only to the consideration of its test section (Fig. 1).

Here the basic elements are silicone pipe, of diameter $D = 18$ mm; hollow rigid narrowings, of various shape and minimum inner diameter $d_{\min}$ and length l (Fig. 2), the movable measuring block, with pressure sensor and needle (for dye injection) flash-mounted into the pipe wall opposite one another. The working medium was water.

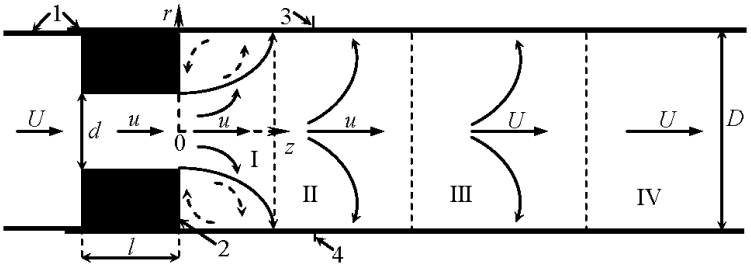

Fig. 1. Schematic of test section:
1 — cut silicone pipe; *2* — narrowing; *3* — pressure sensor; *4* — needle

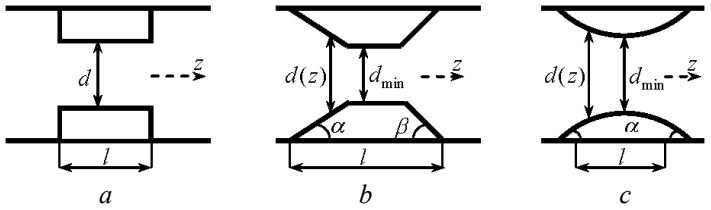

a *b* *c*

Fig. 2. Narrowing shapes:
a —abrupt; *b* — trapezium-like; *c* — streamlined

In the pipe, a flow with controlled characteristics was created. The flow became disturbed in the narrowing and then remained disturbed in a finite region immediately behind it. In this region were the flow separation (I) and flow reattachment (II) zones. Then flow stabilization and recovery back to the basic state upstream of the narrowing were observed (zone III). This region was followed by zone IV in which the flow was like the basic one. The pressure p_t was measured in zones I-III, and two its characteristics studied. These are the *rms* pressure $p_{rms} = \sqrt{< p_t^2 >}$ and the power spectrum P (here the brackets denote an ensemble average).

The mean axial velocity of the basic flow upstream of the narrowing U, was determined from the ratio of the water volume ΔV, accumulated in the collection tank (calibrated in litres) during the period T of data acquisition to the cross-sectional area of the pipe, $\pi D^2/4$, and the time T viz $U = \Delta V / \left(T \pi D^2 / 4 \right)$. The mean axial flow velocity in the narrowing throat u, was found from the mass conservation condition in the most narrowed and normal segments of the pipe viz. $u = U \left(D / d_{\min} \right)^2$ (for the abrupt narrowing $d_{\min} = d$). In order to have similarity in the basic flow Reynolds number, $\mathrm{Re}_D = UD/\nu$, (where ν is the kinematical fluid viscosity) between the experimental flow and real blood flow in a larger vessel, only velocities $U < 0.39$ m/s were considered in the experiment. For these U, one had $\mathrm{Re}_D < 7000$, which is typical of the larger arteries of the human body [2, p. 479; 3, p. 663].

Results

The axisymmetric geometry and coaxial location of the two parts of the pipe and the narrowing resulted in axial symmetry of the test section flow and, hence, axial symmetry of the pressure p_t [3, p. 663].

Pressure p_{rms}

Typical axial distribution of the pressure p_{rms} behind all the narrowings is depicted in Fig. 3.

The data were obtained behind the narrowings of the same severity, S, quantified here as

$$S = \left(1 - d_{\min}^2 / D^2\right) 100\ \%$$

and the same length, l, and at the same value of the basic flow Reynolds number, Re_D.

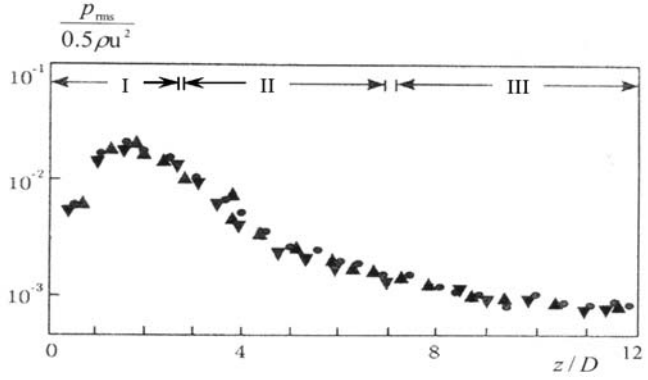

Fig. 3. Axial distribution of the pressure p_{rms} behind a narrowing ($d_{\min} = 5$ мм, $S = 92.28\ \%$, $l = 40$ мм, $U = 0.25$ m/s, $\mathrm{Re}_D = 4500$): • — abrupt narrowing; ▲ — trapezium-like narrowing ($\alpha = \beta = \pi/4$); ▼— streamlined narrowing ($\alpha = \pi/4$)

Pressure p_{rms} behind the abrupt narrowing

Study of the axial variation of the pressure p_{rms} behind the abrupt narrowing shows that it initially increases sharply as the distance z from the narrowing increases, reaching a maximum, $(p_{rms})_{\max}$, at the point $z = L_{\max}$ (this range of z is included in the flow region I). Then p_{rms} decreases rather rapidly and, at the very end of the region III, reaches a minimum, $(p_{rms})_{\min}$, which is equal to the value measured upstream of the narrowing. The lengths L_{I} and $L_{\mathrm{I+II}}$ of the flow separation I and the most disturbed flow I+II regions can be seen from Fig. 3 not to exceed approximately three and seven pipe diameters, respectively, viz. $L_{\mathrm{I}} < 3D$, $L_{\mathrm{I+II}} < 7D$. The axial dimension $L_{\mathrm{I+II+III}}$ of the total disturbed flow region I+II+III is less than $12D$, viz. $L_{\mathrm{I+II+III}} < 12D$. Similar estimates for the lengths L_{I}, $L_{\mathrm{I+II}}$ and $L_{\mathrm{I+II+III}}$ have been obtained for the other parameter values.

Analysis of the pressure p_{rms} and the location of its maximum at $z = L_{\max}$ behind abrupt narrowings of the same length and different severity and/or at various values of Re_D shows that (i) the maximum lies between the narrowing and the flow reattachment point in the range $z/D \approx 1.3 - 2.6$, and moves downstream/upstream as S and(or) Re_D increase/decrease; (ii) an increase/decrease in S and(or) Re_D causes a general increase/decrease of the local disturbed flow energy and, hence, a corresponding general increase/decrease (ranging from a few percents to a few times depending on z and the compared values of S and(or) Re_D) of the pressure p_{rms}.

Variations in the *rms* pressure caused by changes in the narrowing length are much weaker than those due to changes in S and/or Re_D. More specifically, they are generally in that a significant (i.e., around 50 %) increase/decrease in l from the value of 20 mm (for $S > 69\ \%$ and $\mathrm{Re}_D > 1680$) results in (i) an insignificant (i.e., of the order of 5–7 % depending on S and(or) Re_D) shift of the point $z = L_{\max}$ downstream/upstream; (ii) an increase/decrease of the flow energy dissipation in the narrowing (due to the increase/decrease of the viscous forces there) and, consequently, a small (i.e., of the order of 5–10 % depending on z, S and(or) Re_D) decrease/increase of the *rms* pressure.

In order to characterise quantitatively the dependence of the distance $L_{\max}$ on the narrowing severity and the jet Reynolds number, $\mathrm{Re}_d = u d_{\min}/\nu$, it was assumed to take the form

$$L_{\max}/d = A\left(\mathrm{Re}_d\right)^B \left(D/d\right)^C. \qquad (1)$$

In varying the parameters A, B and C in expression (1), it was found that the data for narrowings of differing severities could be reduced to approximately a single curve with the values $A = 0.127$, $B = 0.26$, $C = 1.25$. The relative error coefficient ς, calculated from the expression

$$\varsigma = \sum_{i=1}^{N} \varsigma_i / N ,$$

$$\varsigma_i = \left| 1 - \frac{A\left(\mathrm{Re}_d\right)^B \left(D/d\right)^C}{L_{\max}/d} \right|_{\mathrm{Re}_d=(\mathrm{Re}_d)_i} ,$$

where N is the number of measurements, was equal to 0.115. This indicates a small difference between the experimental values for $L_{\max}$ and those found from formula (1). Consequently, one can conclude that

$$L_{\max}/d \approx 0.127\left(\mathrm{Re}_d\right)^{0.26}\left(D/d\right)^{1.25}. \qquad (2)$$

Estimate (2) indicates that the point $z = L_{\max}$ shifts to the right/left as Re_d and(or) S increase/decrease.

Study of the maximum pressure $(p_{rms})_{\max}$, shows that (like the *rms* pressure throughout the flow domain under investigation) it increases/decreases as S and(or) Re_d increase/decrease. Furthermore, for $\mathrm{Re}_d > 8500$, it is approximately proportional to the jet dynamic pressure, $\rho u^2/2$, and the ratio d/D, viz.

$$\left(p_{\mathrm{rms}}\right)_{\max} / \left(0.5\rho u^2\right) \times \left(D/d\right) \approx 0.054 ,$$
$$\mathrm{Re}_d > 8500 . \qquad (3)$$

Pressure p_{rms} behind the trapezium-like and streamlined narrowings

Analysis of the axial distribution of the rms pressure behind the trapezium-like narrowing, $p_{rms}^{(tr)}$, shows that (Fig. 3) it is similar to that behind the abrupt one, p_{rms}. The difference is that the amplitude of $p_{rms}^{(tr)}$ is generally slightly lower than that of p_{rms}. However, for the parameter values used, this only becomes noticeable (i.e., within a few percent of the relative difference depending on z, S, l, α and Re_D) for $S > 92\%$, $l \le 40$ mm, $\alpha \le \pi/4$ and $\mathrm{Re}_D > 4450$.

Furthermore, the other conditions being equal, (i) the stronger/milder S the more/less significant is the influence of α on the *rms* pressure; (ii) a significant (i.e., around 30^o) increase/decrease in α (for $S > 92\%$, $l \le 40$ mm and $\mathrm{Re}_D > 4450$) causes a general increase/decrease (of the order of 5–7 % depending on z, S, l and Re_D) of $p_{rms}^{(tr)}$ and, hence, a corresponding general decrease/increase of the difference between p_{rms} and $p_{rms}^{(tr)}$.

As for the angle β of the trapezium-like narrowing, its influence on $p_{rms}^{(tr)}$ is insignificant for the chosen variation ranges of the parameters (although theoretically β must influence the appearance/disappearance of the flow separation region, its length (when the region exists), etc.).

A general decrease in the *rms* pressure due to the decrease in α is explained by that the degree of flow disturbance behind a narrowing of more smooth shape is lower than that behind a narrowing of less smooth shape.

Herewith for the used narrowings, the degree is mainly controlled by the angle α. More specifically, a decrease in α (i.e., smoothing of the shape) causes a general decrease of the degree and, hence, a general decrease in the pressure, and vice versa, an increase of α results in a general increase of the degree and, accordingly, a general increase of the pressure.

Practically all the same can be said about the axial distribution of the *rms* pressure behind the streamlined narrowing, $p_{rms}^{(s)}$, (Fig. 3). The difference between $p_{rms}^{(s)}$ and $p_{rms}^{(tr)}$ is that $p_{rms}^{(s)}$ is generally slightly lower than $p_{rms}^{(tr)}$, and, for the parameter values used, this only becomes noticeable (within a few percent of the relative difference depending on z, S, l, α and Re_D) for $S > 92\%$, $l \le 40$ mm, $\alpha \le \pi/4$ and $\mathrm{Re}_D > 4450$.

As above, it is explained by the decrease in the degree of flow disturbance due to smoothing of the narrowing shape.

Study of the variations in the pressures $p_{rms}^{(tr)}$ and $p_{rms}^{(s)}$ caused by changes of S, l and/or Re_D shows that qualitatively they do not differ from the corresponding variations in p_{rms}. Also the quantitative estimates for the distances $L_{\max}^{(tr)}$ and $L_{\max}^{(s)}$ do not practically differ from estimate (2), viz.

$$L_{\max}^{(tr)}/d_{\min} \approx L_{\max}^{(s)}/d_{\min} \approx$$
$$\approx 0.127(\mathrm{Re}_d)^{0.26}\left(D/d_{\min}\right)^{1.25}. \qquad (4)$$

As for the quantitative estimates for the maximum *rms* pressure behind the trapezium-like and streamlined narrowings, their little difference from estimate (3) only becomes noticeable (i.e., within a few percent of the relative difference depending on S, l, α and Re_D) for $S > 92\%$, $l \le 40$ mm, $\alpha \le \pi/4$ and $\mathrm{Re}_D > 4450$, viz.

$$(p_{\mathrm{rms}}^{(tr)})_{\max} / \left(0.5\rho u^2\right)\left(D/d_{\min}\right) \approx$$
$$\approx (p_{rms}^{(s)})_{\max} / \left(0.5\rho u^2\right)\left(D/d_{\min}\right) \approx K, \quad ;$$
$$\mathrm{Re}_d > 8500 ; \qquad (5)$$

$$K \approx \begin{cases} 0.054, & S < 92\,\%, \alpha > \pi/4; \\ K_{tr}(\alpha, S) < 0.054, & S > 92\,\%, \alpha \le \pi/4; \\ K_s(\alpha, S) < K_{tr}(\alpha, S), & S > 92\,\%, \alpha \le \pi/4, \end{cases}$$

(a conclusion concerning the dependencies $K_{tr} = K_{tr}(\alpha, S)$ and $K_s = K_s(\alpha, S)$ may be deduced after carrying out the appropriate experiments).

Wall pressure power spectrum

Typical results for the power spectra of the wall pressure fluctuations behind the abrupt narrowing, as well as behind all the investigated narrowings are presented in Fig. 4 and 5, respectively. The recordings were made in the flow separation I and flow reattachment II regions at the same values of the parameter set $\{S, l, \mathrm{Re}_D\}$.

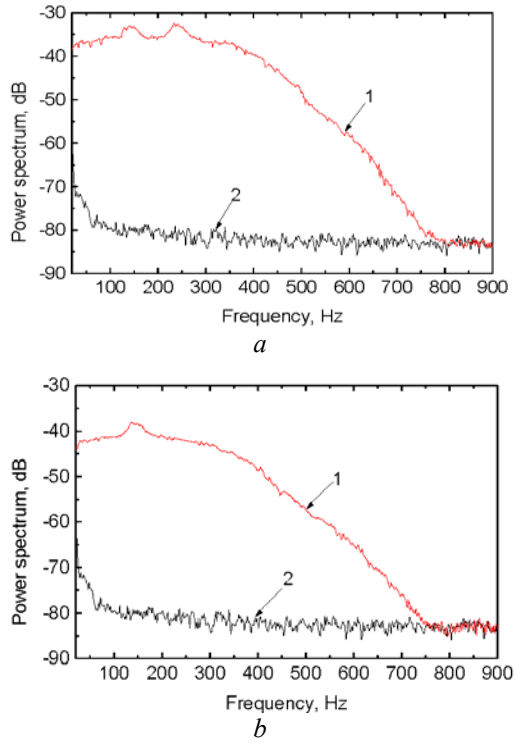

Fig. 4. Power spectrum at (*a*) $z = L_{\max}$ and (*b*) $z = 4D$ behind the narrowing ($d = 10$ mm, $S = 69.14\,\%$, $l = 20$ mm) at $U = 0.35$ m/s ($\mathrm{Re}_D = 6300$): *1* — abrupt narrowing; *2* — background noise

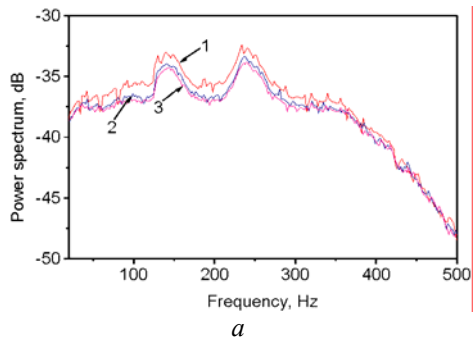

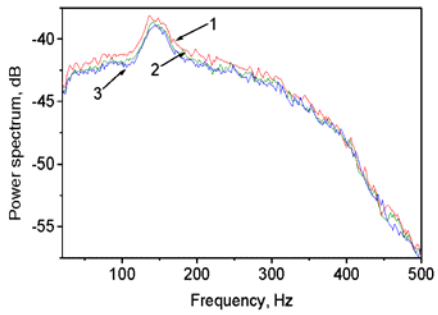

Fig. 5. Power spectrum at (*a*) $z = L_{\max}$ and (*b*) $z = 4D$ behind the narrowing ($d_{\min} = 10$ mm, $S = 69.14\,\%$, $l = 20$ mm) at $U = 0.35$ m/s ($\mathrm{Re}_D = 6300$): *1* — abrupt narrowing; *2* — trapezium-like narrowing ($\alpha = \beta = \pi/3$); *3* — streamlined narrowing ($\alpha = \pi/3$).

Power spectrum behind the abrupt narrowing

Study of the wall pressure power spectrum P behind the abrupt narrowing (see Fig. 4) shows that generally it looks like that of the wall pressure fluctuations in a fully-developed turbulent flow in a pipe without narrowing, P_0, [3, p. 668]. More specifically, the low-frequency domain of P in each flow region is the energy-containing and characterizes the distribution of the disturbed flow energy among the energy-containing large-scale eddies in that region. The high-frequency domain of P corresponds to small-scale eddies which contain a small part of the disturbed flow energy. As a result, here the level is much lower than in the low-frequency domain and decreases rapidly as the frequency increases (corresponding to the decrease in a vortex' energy with the decrease of its size).

A characteristic feature of the spectrum P (compared with P_0, which is a rather smooth function) is that it has local pronounced low-frequency maxima (two in Fig. 4a and one in Fig. 4b). Analysis of the flow structure and the flow energy distribution among the eddies behind the narrowing shows that these maxima are determined by the corresponding large-scale vortex formations in the flow regions I and II, and that the frequencies of the maxima can be attributed to the characteristic frequencies of the vortex formations. More specifically, (i) in region I, these are eddies with sizes of order $d/2$, which move at speeds of order u in the jet and are characterized by frequencies of order

$$f_{ch}^{(1)} = \frac{2u}{d} = \frac{2UD^2}{d^3} \qquad (6)$$

and eddies with scales of order $h = (D - d)/2$ in the recirculating flow region between the jet and the pipe wall, which have frequencies of order

$$f_{ch}^{(2)} = \frac{u_c}{h} \qquad (7)$$

where $u_c \sim 0.45u - 0.6u$ is a convection velocity on the outer side of the jet [3, p. 668]; (ii) in region II, these are vortex formations with sizes of order $D/2$, which are convected at speeds of order u and have frequencies of order

$$f_{ch}^{(3)} = \frac{2u}{D} = \frac{2UD}{d^2}. \qquad (8)$$

As noted in the introduction, it appears that the variation of the wall pressure power spectrum with axial distance from the narrowing has not previously been studied. Comparative analysis of the spectra recorded here at different values of the axial coordinate shows that (see Fig. 4) (i) the local disturbed flow energy decreases as the distance from the narrowing increases, which results in a general decrease in the spectrum level; (ii) the disturbed flow structure and, hence, the number of pronounced low-frequency maxima in the power spectrum change on transiting from the flow separation to the flow reattachment regions.

Study of the spectrum P behind narrowings of differing severity, but with the same length and at equal values of the basic flow Reynolds number shows that (i) the shape of the spectrum is practically independent of S; (ii) the spectrum level generally increases/decreases as S increases/decreases; (iii) the locations of the pronounced low-frequency maxima in the spectrum change with S in accordance with changes in the frequencies (6)–(8).

The first observation arises because the general structure of the disturbed flow and the pressure p_t behind a narrowing does not change significantly with S. The second effect is due to the corresponding increase/decrease in the flow and pressure field energy. The third feature is caused by changes in sizes and/or speeds of the large-scale eddies in the flow regions I and II, and, hence, the corresponding changes of their frequencies $f_{ch}^{(1)}$, …, $f_{ch}^{(3)}$.

The variations in P due to the variations in Re_D are qualitatively similar to those due to changes in S, namely (i) change of Re_D does not significantly affect the shape of P; (ii) increase/decrease of Re_D results in a general increase/decrease in the spectrum level; (iii) change in Re_D causes change of the locations of the low-frequency maxima in P in accordance with changes of the frequencies (6)–(8). The explanation of these effects is similar to that due to changes in S.

Finally, the effect of the narrowing length on the spectrum P is not as significant as that of S or Re_D. More specifically, (i) the shape of P and the locations of its maxima near the frequencies $f_{ch}^{(1)}$, …, $f_{ch}^{(3)}$ are practically insensitive to changes in l; (ii) a significant (i.e., around 50 %) increase/decrease in l about the value of 20mm (at $S > 47\,\%$ and $\mathrm{Re}_D > 1570$) generally results in an insignificant (i.e., up to a few dB depending on z, S, frequency f and(or) Re_D) decrease/increase in the spectrum level.

The insensitivity of the spectrum shape to changes in l can be explained by the corresponding invariance of the general structure of the flow and the wall pressure field behind a narrowing. Invariance of the locations of the low-frequency maxima in P is due to the invariance of sizes and speeds of the large-scale vortex formations in the flow regions I and II with changes in l. The decrease/increase in the spectrum amplitude with an increase/decrease in l is caused by the corresponding increase/decrease of flow energy dissipation in the narrowing due to the increase/decrease of the viscous forces there.

Power spectrum behind the trapezium-like and streamlined narrowings

The power spectrum behind the trapezium-like narrowing, P_{tr}, can be seen from Fig.6 to be similar to P measured at the same locations. The difference is that, in general, P_{tr} has little lower low-frequency levels, and this only becomes noticeable (i.e., within a few percent of the relative difference depending on z, S, l, α, f and Re_D) for $S > 69\,\%$ $l \le 40$ mm, $\alpha \le \pi/3$ and $\mathrm{Re}_D > 4000$. Furthermore, the other conditions being equal, (i) the spectrum level becomes more/less sensitive to change in α as the narrowing severity increases/decreases; (ii) a significant (i.e., around 20^0) increase/decrease in α (for $S > 69\,\%$, $l \le 40$ mm and $\mathrm{Re}_D > 4000$) causes a general increase/decrease (of the order of 5-7 % depending on z, S, l, f and Re_D) of the level of the spectrum P_{tr} and, hence, a corresponding general decrease/increase of the difference between the levels of P_{tr} and P.

As for the angle β of the trapezium-like narrowing, its influence on P_{tr} was found to be insignificant for the chosen variation ranges of the experimental parameters.

The similarity of the spectra P_{tr} and P can be explained by the similarity of both the disturbed flow structure and the flow energy distribution among the eddies behind the trapezium-like and abrupt narrowings of the same severity and the same

length, and at the same Reynolds number value. A general decrease of the spectral level with smoothing of the narrowing geometry is due to the corresponding decrease of the degree of flow disturbance behind a narrowing. The explanation of the other effects, which are caused by the noted change in the narrowing shape, is also similar to that in the *rms* pressure.

Practically all the same can be said about the power spectrum behind the streamlined narrowing, P_s, (Fig. 5). The difference between P_s and P_{tr} is that the low-frequency level of P_s is generally slightly lower than that of P_{tr}, and this only becomes noticeable (within a few percent of the relative difference depending on z, S, l, α, f and Re_D) for $S > 69\,\%$, $l \le 40$ mm, $\alpha \le \pi/3$ and $\mathrm{Re}_D > 4000$. Again, it is due to a general decrease in the degree of flow disturbance with smoothing of the narrowing shape. (Here from the comparison of the variations in the power spectrum due to smoothing of the narrowing geometry with those in the *rms* pressure measured at the same axial location, one comes to the conclusion that the spectrum is more sensitive to the noted smoothing than the *rms* pressure. Similar conclusion can be made from the comparison of the variations in the power spectrum and the *rms* pressure due to changes in S, l and Re_D).

Finally, consideration of the variations in the spectra P_{tr} and P_s due to changes of S, l, Re_D, and/or z shows that generally they are similar to the corresponding variations in the spectrum P.

Practical implication of the results

The results of this study can be practically applicable in developing non-invasive diagnostic techniques for vascular stenosis detection. For example, the low-frequency maxima in the power spectrum downstream of the narrowing, found in this study, can also be detected in the power spectrum of both the wall pressure fluctuations after a vascular stenosis, P_t, and the acoustic field, P_{ac}, generated by a stenosed vessel. The latter follows from the general relationship between P_t and P_{ac}, viz. [2, p. 494; 3, p. 671] $P_{ac} = T_b \times P_t$ where T_b is the transfer function which describes sound generation by the source P_t and sound transmission from the source to the body surface. The appearance of such maxima in the spectra P_t and P_{ac} associated with an originally healthy vessel would indicate a local reduction in the lumen area of vessel. Further increases (during the monitoring of the patient) in the spectrum levels and shifts (to higher frequencies) of some of the low-frequency peaks in the spectra P_t and P_{ac} would imply progression in the stenosis severity. At this stage, the correlations between the frequencies of the low-frequency maxima and the experimental parameters (expressions (6)–(8)) can be used to find a first approximation to the minimum stenosis diameter. The calculation proceeds as follows. Firstly, it is necessary to relate the frequencies of maxima in the spectrum P_{ac} (or P_t) to the basic characteristic frequencies identified in this work (i.e., $f_{ch}^{(1)}$, …, $f_{ch}^{(3)}$). Then, if the flow velocity U in the investigated vessel is known, the minimum stenosis diameter can be approximately determined either from (6) or (8), namely $d_{\min} \propto \left(2UD^2 / f_{ch}^{(1)}\right)^{1/3}$, $d_{\min} \propto \left(2UD / f_{ch}^{(3)}\right)^{1/2}$. If U is unknown, $d_{\min}$ can be found, for example, from the system of equations (6) and (8), namely $d_{\min} \propto \left(f_{ch}^{(3)} / f_{ch}^{(1)}\right) D$. Other pairings of equations (6), (7) and (8) will give us additional approximate estimates for the minimum stenosis diameter. The real value of $d_{\min}$ should be close to these estimates.

There can exist cases when the longitudinal dimension of a mild, but detectable, vessel narrowing grows with time, and the narrowing severity remains unchanged. This can lead to a decrease in the levels of the spectra P_t and P_{ac}, and hence to reduced differences with the corresponding recordings made when the vessel was healthy. Consequently, there can exist situations when, on reaching some critical value of stenosis length, $l = l_{cr}$, the difference between noise levels from the healthy and diseased vessels becomes so small that a previously detectable stenosis becomes practically undetectable by basic acoustic diagnosis techniques. The only remaining signs of a stenosis may now be the low-frequency spectral maxima near the frequencies (6)–(8), if distinguishable. If even these maxima cannot be observed, a vascular narrowing cannot then be detected. These considerations suggest that researchers should attempt to establish the quantitative relationship between l_{cr} and the parameters of the flow, vessel and stenosis.

The increase in level of the spectrum P_t, and hence also of the spectrum P_{ac}, due to an increase in the basic flow Reynolds number suggests that it may be easier to detect stenoses under elevated flow conditions (manual labour) rather than under normal flow conditions (patient at rest).

In the study of stenosis hydrodynamics, the concept of a 'critical' stenosis is used, with the critical stenosis S_{cr}, usually interpreted as one for

which a small further reduction in lumen area will cause significant changes in the characteristics of the hydrodynamic field. Typically [2, p. 495; 3, p. 672], it is found that the values for S_{cr} vary widely (50–90 %) depending on the patient. In this series of experiments, it was possible to detect milder narrowings for which $S \approx 20\,\%$. This may be a reason for introducing the 'critical' stenosis into the study of acoustic diagnosis techniques, and might therefore stimulate researchers into finding the quantitative relationships between S_{cr} and the parameters of the stenosis, vessel and flow.

Conclusions

The results obtained in this study and their analysis permit the following conclusions to be drawn.

1. A pipe narrowing disturbs the flow, resulting in a sharp increase of the wall pressure fluctuations in a finite domain immediately behind the narrowing. In this domain, the flow separation (I) and flow reattachment (II) regions, and then the flow stabilization region (III) are observed.

2. The length of the regions I and I+II does not exceed approximately $3D$ and $7D$, respectively, whereas the length of the region I+II+III is less than $12D$ for all the narrowing shapes used.

3. For all the narrowings, the pressure p_{rms} reaches a maximum at a location that is always before the flow reattachment point. Herewith the distance $L_{\max}$ from the narrowing to the point of maximum pressure p_{rms} lies in the range $1.3D - 2.6D$. This distance increases/decreases as the jet Reynolds number, Re_d, and(or) the narrowing severity, S, increase/decrease in accordance with estimates (2) and (4).

4. For $\mathrm{Re}_d > 8500$ behind all the narrowings, the maximum pressure p_{rms} is approximately proportional to the jet dynamic pressure behind the narrowing and the ratio of the diameters of the most narrowed and normal segments of the pipe (see estimates (3) and (5)).

5. The pressure p_{rms} increases/decreases as the narrowing severity, S, and(or) the flow Reynolds number, Re_D, increases/decreases. The pressure weakly decreases/increases with an increase/decrease of the narrowing length l.

6. The power spectrum P in the flow region I+II generally looks like that of the wall pressure fluctuations in a fully-developed turbulent flow in a pipe without narrowing. A characteristic feature of P is that it has pronounced low-frequency maxima. These maxima are associated with large-scale vortex structures in the regions I and II, and their frequencies match the characteristic frequencies of these vortex structures (see expressions (6)–(8)).

7. The shape of the spectra P, P_{tr} and P_s does not depend significantly on S and(or) Re_D; their levels generally increase/decrease as S and(or) Re_D increases/decreases; and the locations of their low-frequency maxima change with changes in these parameters in accordance with (6)–(8). An increase/decrease of the narrowing length causes a weak decrease/increase in the levels of the spectra.

8. The overall level and the number of low-frequency maxima in the power spectrum decrease as the distance from the narrowing increases (i.e., when transiting from the flow separation to flow reattachment regions).

9. Smoothing of the narrowing shape results in a weak decrease of both the pressure p_{rms} and the low-frequency level of the power spectrum.

10. The spectrum P has more characteristic features indicating changes in the narrowing shape than the pressure p_{rms} and these features in P are more sensitive to the noted changes than those in p_{rms}.

REFERENCES

1. **Berger S. A**. Flows in stenotic vessels / S. A. Berger, L.-D. Jou // Ann. Rev. Fluid Mech. — 2000. — 32. — P. 347-382, doi: 10.1146/annurev.fluid.32.1.347. (eng.)

2. **Borisyuk A. O.** Experimental study of noise produced by steady flow through a simulated vascular stenosis / A. O. Borisyuk // J. Sound Vibr. — 2002. — 256. — P. 475-498, doi:10.1006/jsvi.5001. (eng.)

3. **Borisyuk A. O.** Experimental study of wall pressure fluctuations in rigid and elastic pipes behind an axisymmetric narrowing / A. O. Borisyuk // J. Fluids Str. — 2010. — 26, no. 4. — P. 658-674, doi: 10.1016/j.jfluidstructs.2010.03.005. (eng.)

Borysyuk A. O. , Borysyuk Ya. A.

ALL PRESSURE FLUCTUATIONS BEHIND A PIPE NARROWING OF VARIOUS SHAPES

Wall pressure fluctuations behind a pipe narrowing of the abrupt, trapezium-like and streamlined axisymmetric shapes are studied experimentally. A sharp increase in their rms level in a finite region immediately downstream of the narrowing, leading up to a pronounced maximum upstream of the point of jet re-attachment, is found. Approximate estimates for the upper limits of the lengths of that region and its typical domains, as well as quantitative relationships

both for the distance from the narrowing to the point of maximum rms pressure and for the rms magnitude at this point are obtained for all the shapes. Inspection of the wall pressure power spectrum reveals the presence of a few pronounced low-frequency maxima for all the narrowing shapes. The maxima are found to be associated with the large-scale eddies in the domains of separated and reattached flow, and their frequencies are close to the characteristic frequencies of the eddies' formation. These maxima are the main distinguishing features of the spectrum under investigation compared to the power spectrum of the wall pressure fluctuations in a fully-developed turbulent flow in a pipe without narrowing. Study of the narrowing shape effects reveals the appropriate changes in the investigated statistical characteristics of the pressure, the power spectrum being more sensitive to the changes in the shape parameters compared to the rms pressure. Recommendations about possible practical application of the obtained results are given.

Keywords: pipe; narrowing; disturbed flow; wall pressure fluctuations.

Борисюк А. О., Борисюк Я. А.

ПУЛЬСАЦІЇ ПРИСТІННОГО ТИСКУ ЗА ЗВУЖЕННЯМ ТРУБИ РІЗНИХ ФОРМ

Експериментально досліджено пульсації пристінного тиску в трубі за осесиметричними звуженнями обривної, трапецієподібної та обтічної форм. Виявлено різке зростання їх середньоквадратичного значення у скінченному регіоні безпосередньо за звуженням, яке досягає максимуму перед точкою приєднання струменя. Для всіх форм звуження одержано наближені оцінки для верхніх меж довжин цього регіону і його типових областей, а також кількісні співвідношення для відстані від звуження до точки максимуму середньоквадратичного тиску та значення тиску в цій точці. Вивчення спектра потужності виявляє наявність у ньому низькочастотних максимумів. Вони асоціюються з великомасштабними вихорами в областях відривної та приєднаної течії, а їх частоти близькі до характерних частот формування цих вихорів. Ці максимуми є основною особливістю спектра у порівнянні зі спектром потужності пульсацій пристінного тиску у повністю розвиненій турбулентній течії в трубі без звуження. Дослідження ефектів форми звуження виявляє відповідні зміни у статистичних характеристиках пульсацій тиску. При цьому спектр потужності є чутливішим до змін параметрів форми порівняно із середньоквадратичним тиском. Подано рекомендації стосовно можливого практичного застосування одержаних результатів.

Ключові слова: труба; звуження; збурена течія; пульсації пристінного тиску.

Борисюк А. А., Борисюк Я. А.

ПУЛЬСАЦИИ ПРИСТЕНОЧНОГО ДАВЛЕНИЯ ЗА СУЖЕНИЕМ ТРУБЫ РАЗНЫХ ФОРМ

Экспериментально исследуются пульсации пристеночного давления в трубе за осесимметрическими сужениями обрывной, трапециеобразной и обтекаемой форм. Выявлено резкое увеличение их среднеквадратичного значения в конечном регионе непосредственно за сужением, которое достигает максимума перед точкой присоединения струи. Для всех форм сужения получены приближенные оценки для верхних пределов длин этого региона и его типичных областей, а также количественные соотношения для расстояния от сужения до точки максимума среднеквадратичного давления и значения давления в этой точке. Изучение спектра мощности выявляет наличие в нем низкочастотных максимумов. Они ассоциируются с крупномасштабными вихрями в областях отрывного и присоединенного течения, а их частоты близки к характерным частотам формирования этих вихрей. Эти максимумы являются основной особенностью спектра по сравнению со спектром мощности пульсаций пристеночного давления в полностью развитом турбулентном течении в трубе без сужения. Исследование эффектов формы сужения выявляет соответствующие изменения в статистических характеристиках пульсаций давления. При этом спектр мощности является более чувствительным к изменениям параметров формы по сравнению со среднеквадратичным давлением. Даются рекомендации относительно возможного практического применения полученных результатов.

Ключевые слова: труба; сужение; возмущенное течение; пульсации пристеночного давления.

Стаття надійшла до редакції 23.03.2017 р.
Прийнято до друку 24.03.2017 р.
Рецензент – д-р ф.-м. н., проф. Городецька Н. С.